



Imaging findings of solitary uterine granulocytic sarcoma

Aya Yamane¹, Tetsuro Sekine¹, Tadashi Machida¹,
Ikuko Omori², Munehiko Onda³ and Shin-ichiro Kumita¹

Abstract

A 29-year old woman with a history of vaginal bleeding was referred to our hospital. Transvaginal ultrasonography revealed a hypervascular cervical mass and malignancy was suspected. Computed tomography (CT), magnetic resonance imaging, and 18-F-fluorodeoxyglucose positron emission tomography/CT were performed. She was finally diagnosed with granulocytic sarcoma based on pathological examination.

Keywords

Granulocytic sarcoma, uterus, ultrasound, computed tomography (CT), magnetic resonance imaging (MRI), positron emission tomography/computed tomography (PET/CT)

Date received: 1 March 2017; accepted: 5 March 2017

Introduction

Granulocytic sarcoma (GS) is a rare solid extramedullary tumor composed of immature leukocytes and commonly associated with acute myelogenous leukemia (AML) (1–3). Solitary GS of the uterus is extremely rare. Here, we report the imaging findings of a patient with solitary uterine GS without AML.

Case report

A 29-year-old woman with a history of vaginal bleeding was referred to the Department of Gynecology in our hospital. Transvaginal ultrasonography revealed a hypervascular cervical mass with a diameter of about 5 cm (Fig. 1). Workup was performed using dynamic computed tomography (CT), contrast-enhanced magnetic resonance imaging (MRI), and 18-F-fluorodeoxyglucose (18F-FDG) positron emission tomography/CT (PET/CT). The dynamic CT images showed gradual enhancement (Fig. 2). Compared with the muscle tissue, the mass was isointense on T1W images (Fig. 3a), and mildly hyperintense on T2W images (Fig. 3b and c). Contrast-enhanced fat-suppressed T1W images revealed homogeneous enhancement (Fig. 3d). The value of apparent diffusion coefficient (ADC) map showed strongly restricted diffusion ($0.43 \times 10^{-3} \text{mm}^2/$

s) (Fig. 3e). Homogenous uptake was observed in PET images with maximum standardized uptake value (SUVmax) of 3.78 (Fig. 4a). No other abnormal uptake was observed (Fig. 4b). Malignant lesion was suspected based on these findings. Pathological examination of the biopsy specimens revealed atypical myeloperoxidase-positive cells diffusely infiltrating to the cervical stroma, which confirmed the diagnosis of GS (Fig. 5). A bone marrow examination revealed the absence of leukemia. The patient was referred to a hematologist and chemotherapy was performed according to the AML regimen. Complete response was obtained after the first treatment.

Discussion

GS is a rare solid extramedullary tumor composed of immature leukocytes with an incidence of about two per million. It is commonly associated with AML,

¹Department of Radiology, Nippon Medical School, Tokyo, Japan

²Department of Hematology, Nippon Medical School, Tokyo, Japan

³Department of Pathology, Nippon Medical School, Tokyo, Japan

Corresponding author:

Aya Yamane, Department of Radiology, Nippon Medical School, 1-1-5 Sendagi, Bunkyo-ku, Tokyo 113-0023, Japan.
Email: aya0729@nms.ac.jp



and generally appears concurrently with AML or after treatment (2,3). GS can involve many different organs, such as bone, the lymph nodes, gastrointestinal tract, lung, mediastinum, breast, nasopharynx, and skin (1–3). Solitary uterine GS is very rare and there are few reports on its imaging findings.

Shinagare et al. reported that, compared to muscle, the signal of GS was isointense (75.6%) on T1W images and mildly hyperintense (95.1%) on T2W images, and had homogeneous enhancement (76.3%) in 69 cases (3); we found similar signal characteristics in the present case.

PET/CT can be another option for imaging. Increased FDG uptake is commonly observed in GS as well as other malignant tumors (1,2). However,

Ueda et al. reported that SUVmax was in the range of 2.6–9.7 in seven cases of GS in PET/CT (2), thus SUVmax alone might not be useful for the diagnosis of GS.

Our imaging findings were compatible with the pathological findings. The strongly restricted diffusion on the ADC map and the high density of the mass in non-enhanced CT (48 HU) suggested high cellularity of the mass (Figs. 2a and 3e), which was confirmed via pathological examination. Neither necrosis nor destruction of the histological architecture was observed in the images despite the large tumor size. Pathological examination showed diffuse infiltration of atypical cells, preserving the glandular structure of the uterus (Fig. 5a).

The differential diagnosis involves various malignant tumors, including cervical cancer, sarcoma, neuroendocrine tumor, and malignant lymphoma (ML). The absence of necrosis and destruction of the surrounding structure is not typical of malignant epithelial tumor or sarcoma. On the other hand, the homogeneous enhancement and high cellularity are suggestive of ML. Because GS has the same features, it is difficult to distinguish ML from GS.

In conclusion, there are few specific features for GS and pathological examination is mandatory for confirmative diagnosis. However, the present case demonstrates that image findings can reflect pathological features. Therefore, GS can be included into differential diagnoses by careful observation of various imaging modalities.

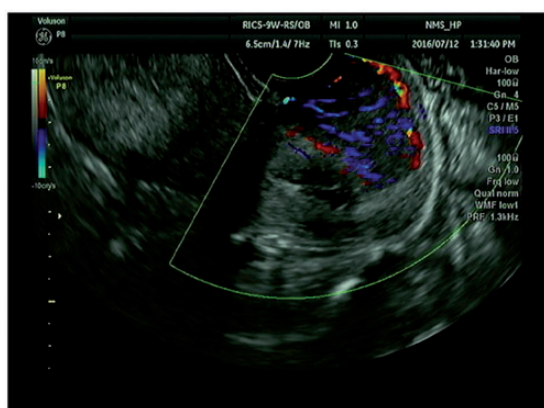


Fig. 1. Transvaginal ultrasonography showed a hypervascular mass.

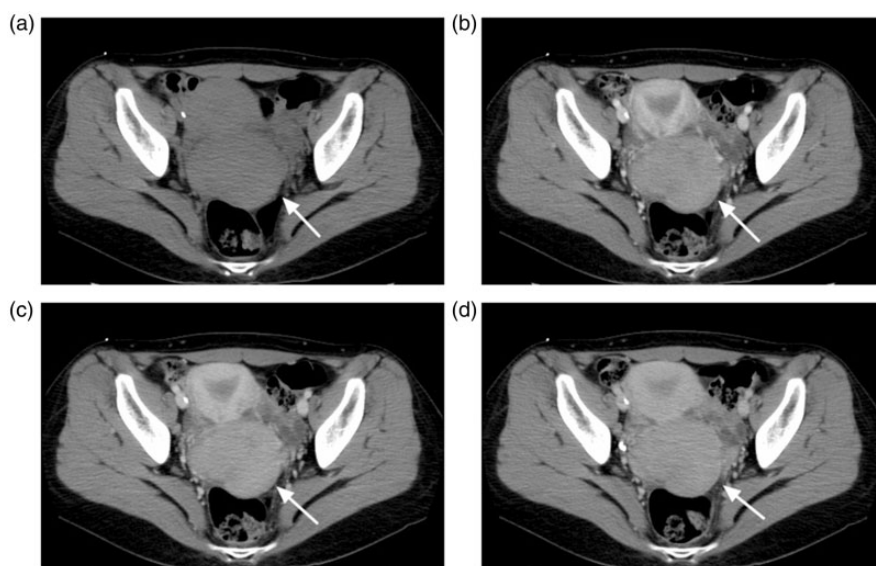


Fig. 2. Dynamic CT images: (a) non-enhanced, (b) arterial phase, (c) portal phase, (d) equilibrium phase. Dynamic CT showed gradual enhancement. Non-enhanced CT revealed a high-density mass (48 HU).

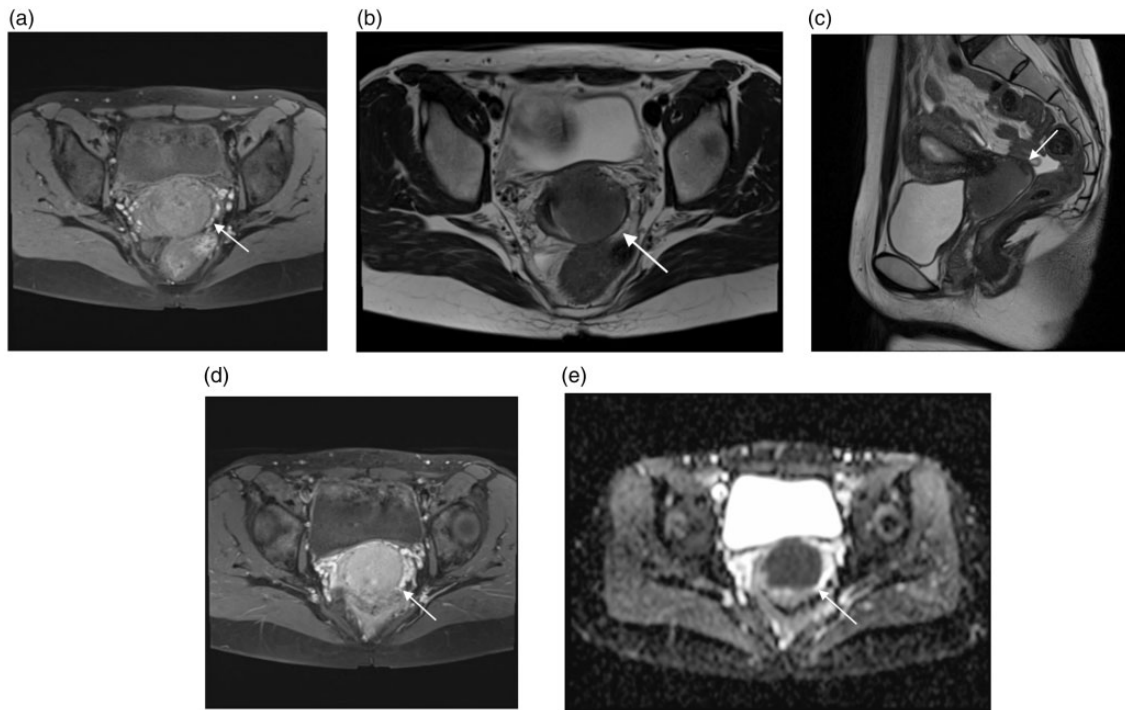


Fig. 3. Contrast-enhanced MRI: (a) axial fat-suppressed T1W images, (b) axial T2W images, (c) sagittal T2W images, (d) contrast-enhanced fat-suppressed T1W images, (e) ADC map. T1W and T2W images showed an isointense mass confined to the cervix, and contrast-enhanced fat suppressed T1W images revealed homogeneous enhancement. The ADC map showed strongly restricted diffusion ($0.43 \times 10^{-3} \text{ mm}^2/\text{s}$).

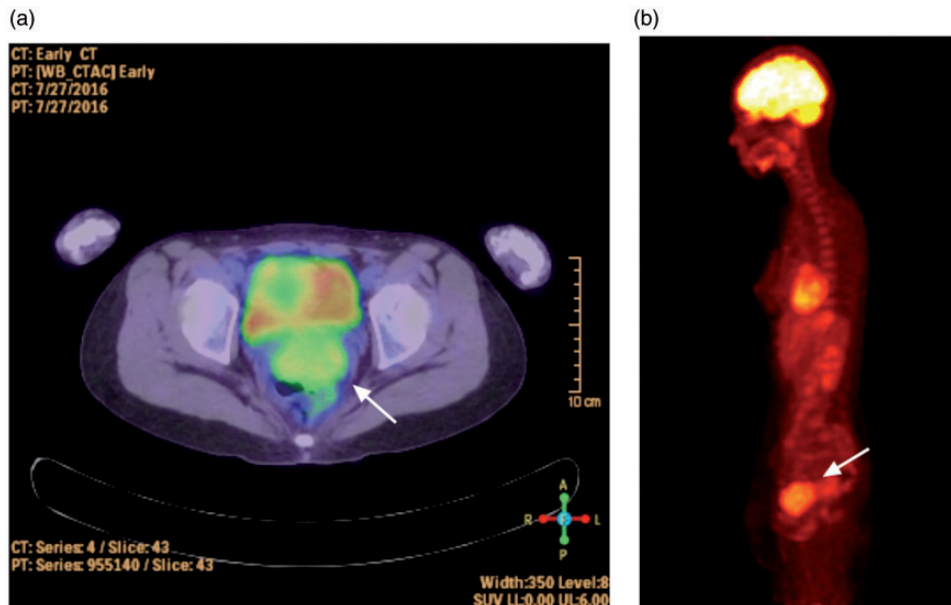


Fig. 4. ^{18}F -FDG PET/CT: (a) axial PET/CT, (b) lateral MIP image. Homogenous uptake was observed in the PET/CT images with maximum standardized uptake value (SUVmax) of 3.78. No distal lesion was observed.

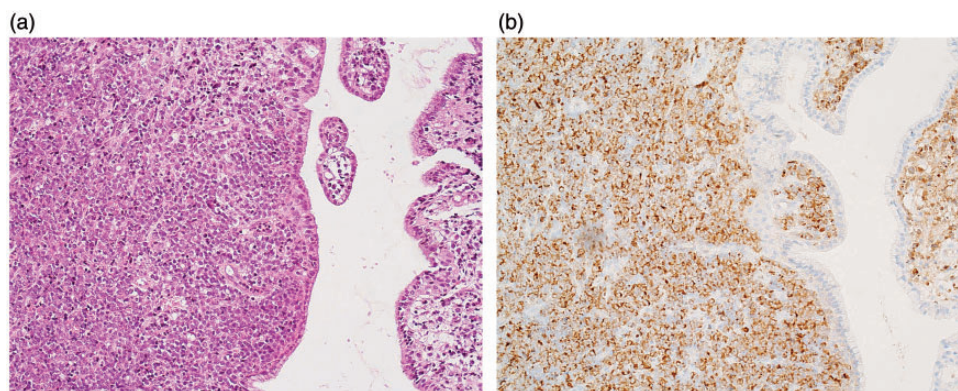


Fig. 5. Pathological examination microscopy images: (a) hematoxylin-eosin 200 \times , (b) myeloperoxidase 200 \times .

Declaration of conflicting interests

The author(s) declared no potential conflicts of interest with respect to the research, authorship, and/or publication of this article.

Funding

The author(s) received no financial support for the research, authorship, and/or publication of this article.

References

1. Zheng LC, Ouyang XL, Zhang WJ, et al. ^{18}F -FDG PET/CT of primary cervical granulocytic sarcoma. *Clin Nucl Med* 2015;40:917–918.
2. Ueda K, Ichikawa M, Takahashi M, et al. FDG-PET is effective in the detection of granulocytic sarcoma in patients with myeloid malignancy. *Leuk Res* 2010;34:1239–1241.
3. Shinagare AB, Krajewski KM, Hornick JL, et al. MRI for evaluation of myeloid sarcoma in adults: a single-institution 10-year experience. *Am J Roentgenol* 2012;199:1193–1198.